Nanotechnology Perceptions
ISSN 1660-6795
www.nano-*ntp.com*

Half-Metallic Ferromagnetism In Cr- And V-Doped Cdn And Znn: A First-Principles Study For Spintronic Applications

Lalmuanawma Chhangte[1], Lalnunpuia[2,*], Lalrintluanga Sailo[3], Lawrence Zonunmawia[3], Remlalsiama[3], Zaithanzauva Pachuau[4], Malsawmtluanga[5], T Malsawmtluanga[1]

[1]Department of Physics, Lunglei Govt. College, Lunglei, Mizoram, India
[2]Department of Physics, Govt. Champhai College, Champhai, Mizoram, India
[3]Department of Physics, Govt. Zirtiri Res. Sc. College, Aizawl, Mizoram, India
[4]Department of Physics, Mizoram University, Aizawl, Mizoram, India
[5]Research Scholar, Mizoram University, Aizawl, Mizoram, India
[*]Corresponding Author: lnpuia@gmail.com

The electronic and magnetic properties of Cr- and V-doped CdN and ZnN were investigated using first-principles calculations based on density functional theory within the GGA and GGA+U frameworks. Structural optimization confirms that all doped compounds are stable in the cubic rock salt phase. The results show that Cr doping induces half-metallic ferromagnetism in both CdN and ZnN, characterized by metallic behavior in the majority spin channel and a finite band gap in the minority spin channel, leading to 100% spin polarization. In contrast, V-doped systems exhibit metallic behavior in both spin channels with reduced spin polarization. The inclusion of Hubbard U enhances the band gap and magnetic moments in Cr-doped compounds, indicating the importance of electron correlation effects. These findings suggest that Cr-doped CdN and ZnN are promising candidates for spintronic applications.

Keywords: Density functional theory; Half-metallicity; Spintronics; Transition metal doping; Magnetic properties.

1. Introduction

The rapid development of spintronics has significantly transformed modern electronics by introducing the possibility of exploiting both the charge and spin degrees of freedom of electrons. Unlike conventional electronic devices, which rely solely on charge transport, spintronic devices utilize spin-polarized currents, offering advantages such as non-volatility, faster switching speeds and reduced power consumption [1]. A key requirement for efficient spintronic applications is the availability of materials capable of producing highly spin-polarized carriers.

Among the different classes of materials investigated, half-metallic ferromagnets (HMFs) have attracted considerable attention due to their unique electronic structure, in which one spin channel exhibits metallic conductivity while the other behaves as a semiconductor or insulator. This leads to complete spin polarization at the Fermi level, making such materials ideal for

spin injection and detection in spintronic devices [2]. The concept of half-metallicity was first proposed in Heusler alloys, which demonstrated the possibility of achieving 100% spin polarization through band structure engineering [3]. Since then, extensive research has been directed toward discovering new half-metallic systems with improved stability and compatibility with semiconductor technologies [4].

Dilute magnetic semiconductors (DMS), formed by introducing transition metal impurities into non-magnetic semiconductors, represent an important class of materials for achieving spin-dependent electronic properties. The incorporation of transition metal atoms introduces localized d-electron states that interact with the host lattice, leading to exchange splitting and magnetic ordering [5]. In this context, binary nitrides such as CdN and ZnN are particularly interesting due to their structural stability and potential for electronic tunability. Experimental studies have reported that ZnN can exhibit semiconducting behavior with varying band gap values depending on growth conditions [6,7], while theoretical investigations suggest that CdN may exhibit narrow band gap semiconducting or even metallic characteristics [8].

The introduction of transition metal dopants such as chromium (Cr) and vanadium (V) into these host materials can significantly alter their electronic and magnetic properties. The interaction between the localized d-states of the dopants and the p-states of nitrogen leads to strong p-d hybridization, which plays a crucial role in determining the magnetic exchange interactions and electronic band structure [9]. Previous studies have shown that Cr doping tends to induce strong ferromagnetism and half-metallicity in several semiconductor systems, whereas V doping often results in weaker magnetic ordering and predominantly metallic behavior [10,11].

From a computational perspective, density functional theory (DFT) has become an essential tool for investigating the electronic and magnetic properties of materials at the atomic scale. However, standard approximations such as the generalized gradient approximation (GGA) often fail to accurately describe systems with strongly correlated d-electrons, leading to underestimated band gaps and magnetic interactions. To address this limitation, the DFT+U approach is employed to incorporate on-site Coulomb interactions, providing a more accurate description of electron localization and exchange effects in transition metal systems [12].

Despite the considerable progress in understanding transition metal doped semiconductors, a systematic investigation comparing the effects of Cr and V doping in CdN and ZnN, particularly at higher doping concentrations and within the DFT+U framework, remains limited. Furthermore, the influence of electron correlation on half-metallicity and magnetic properties in these materials is not yet fully understood. In this work, a comprehensive first-principles study is carried out to analyze the electronic structure, magnetic behavior and spin polarization of Cr- and V-doped CdN and ZnN. Special attention is given to the origin of half-metallicity, the role of p-d hybridization, and the effect of Hubbard U on the electronic and magnetic properties of these systems.

2. Computational Methodology

The electronic and magnetic properties of Cr- and V-doped CdN and ZnN compounds were investigated using the full-potential linearized augmented plane wave (FP-LAPW) method within the framework of density functional theory (DFT) [13,14]. The calculations were carried out using the WIEN2k simulation package, which implements the FP-LAPW method

with no shape approximation to the charge density or potential [15-17]. The exchange-correlation effects were treated within the generalized gradient approximation (GGA) as proposed by Perdew and co-workers [18-20].

To properly describe the strong electron correlation effects associated with the localized 3d electrons of transition metal dopants, the Hubbard U correction (DFT+U) was applied to the Cr-doped systems. The on-site Coulomb interaction parameter U was considered as 2.3 eV, 5.0 eV and 6.0 eV, while the exchange parameter J was taken as zero. This approach improves the description of orbital-dependent interactions and provides a more reliable estimation of band gaps and magnetic properties.

Within the FP-LAPW framework, the Kohn-Sham orbitals are expanded in atomic-like functions inside the muffin-tin spheres and plane waves in the interstitial region. Core electrons were treated relativistically, whereas valence electrons were treated using a semi-relativistic approximation. The basis set size was controlled by the parameter $R_{MT}K_{max}$, which was set to 7.0. The self-consistent field (SCF) calculations were considered converged when the total energy difference between successive iterations was less than 10^{-4} Ry.

The parent compounds CdN and ZnN crystallize in the NaCl-type rock salt structure with cubic symmetry belonging to the $Fm\bar{3}m$ space group. The optimized lattice constants for the primitive unit cells were found to be 4.72 Å for CdN and 4.50 Å for ZnN. To simulate doping effects, 2×2×2 supercells containing eight formula units (M_8N_8, where M = Cd or Zn) were constructed. Transition metal atoms (Cr and V) were substituted at the cation sites to achieve a doping concentration of 37.5%, resulting in compositions $Cd_{0.625}Cr_{0.375}N$, $Cd_{0.625}V_{0.375}N$, $Zn_{0.625}Cr_{0.375}N$, and $Zn_{0.625}V_{0.375}N$.

The muffin-tin radii (R_{MT}) were chosen as 1.52 Å for Cd, 1.37 Å for Zn, 1.26 Å for Cr and V and 0.74 Å for nitrogen. Brillouin zone integrations were performed using a Monkhorst-Pack k-point mesh consisting of 63 k-points for the supercell calculations [21]. This choice ensures a good balance between computational accuracy and efficiency.

Spin-polarized calculations were carried out for all systems to investigate their magnetic and electronic properties. Both spin-up and spin-down channels were explicitly considered to analyze spin polarization and half-metallic behavior. The electronic band structures, density of states (DOS) and magnetic moments were computed for all doped systems using both GGA and GGA+U methods to assess the influence of electron correlation effects.

3. Crystal Structure and Volume Optimization

The structural properties of the transition metal doped compounds $Cd_{0.625}Cr_{0.375}N$, $Cd_{0.625}V_{0.375}N$, $Zn_{0.625}Cr_{0.375}N$, and $Zn_{0.625}V_{0.375}N$ were investigated to determine their equilibrium configurations and structural stability. The parent compounds CdN and ZnN crystallize in the rock salt (NaCl-type) structure with cubic symmetry belonging to the $Fm\bar{3}m$ space group. To simulate the effect of doping, 2×2×2 supercells were constructed, and substitution of cation sites by Cr and V atoms was carried out to achieve a doping concentration of 37.5%.

The equilibrium lattice parameters were obtained by minimizing the total energy of the system as a function of unit cell volume. The calculated energy–volume data were fitted using the third-order Birch–Murnaghan equation of state [22] expressed as:

$$E(V) = E_0 + \frac{9V_0B_0}{16}\left[\left\{\left(\frac{V_0}{V}\right)^{2/3} - 1\right\}^3 B_0' + \left\{\left(\frac{V_0}{V}\right)^{2/3} - 1\right\}^2 \left\{6 - 4\left(\frac{V_0}{V}\right)^{2/3}\right\}\right]$$

where E_0, V_0, B_0 and B_0' represent the equilibrium energy, equilibrium volume, bulk modulus and its pressure derivative respectively. The fitted energy-volume curves for $Cd_{0.625}Cr_{0.375}N$ and $Zn_{0.625}Cr_{0.375}N$ are shown in Fig. 1, which exhibit clear minima indicating stable ground-state configurations.

Fig 1: Total energy versus volume curves and stability analysis of (a) $Cd_{0.625}Cr_{0.375}N$ and (b) $Zn_{0.625}Cr_{0.375}N$ using GGA and GGA+U approaches.

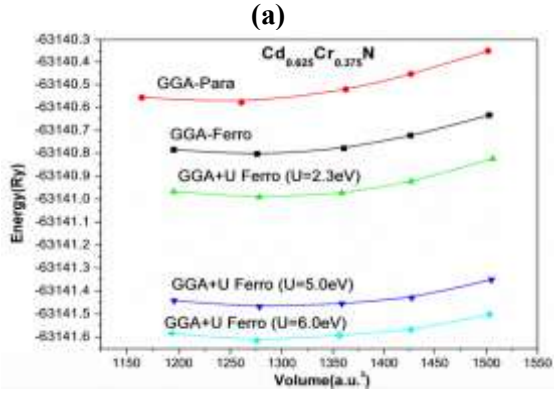

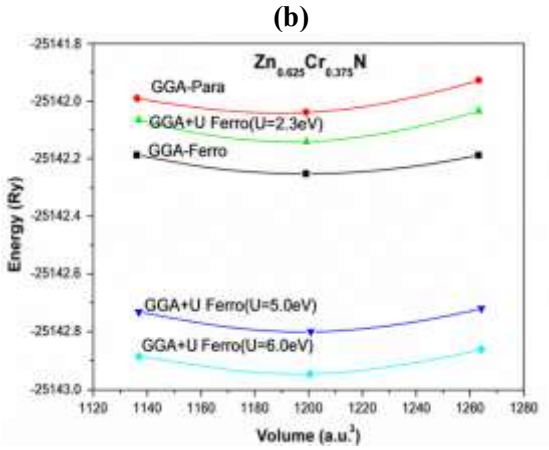

The optimized lattice parameters obtained from these calculations show only slight deviations compared to the pristine CdN and ZnN systems. A comparison between GGA and GGA+U results reveals that the inclusion of the Hubbard U parameter leads to a marginal decrease in lattice constants. This behavior can be attributed to enhanced localization of d-electrons, which

slightly modifies the bonding interactions within the crystal [23]. However, no structural phase transition is observed and the cubic symmetry is preserved in all cases.

Table 1: Calculated lattice parameters (Å) of doped CdN and ZnN in GGA and GGA+U methods

Compound	GGA	GGA+U (U = 2.3 eV)	GGA+U (U = 5.0 eV)	GGA+U (U = 6.0 eV)
$Cd_{0.625}Cr_{0.375}N$	4.73	4.64	4.69	4.69
$Cd_{0.625}V_{0.375}N$	4.73	-	-	-
$Zn_{0.625}Cr_{0.375}N$	4.50	4.34	4.50	4.50
$Zn_{0.625}V_{0.375}N$	4.50	-	-	-

The calculated lattice constants for the doped systems are summarized in Table 1. It is evident that the lattice parameters remain nearly unchanged across different doping configurations and computational approaches, confirming the structural robustness of the host lattice upon substitution.

Fig 2: Crystal structure representations of (a) $Cd_{0.625}Cr_{0.375}N$, (b) $Cd_{0.625}V_{0.375}N$, (c) $Zn_{0.625}Cr_{0.375}N$, and (d) $Zn_{0.625}V_{0.375}N$, showing atomic arrangements along the a-b plane.

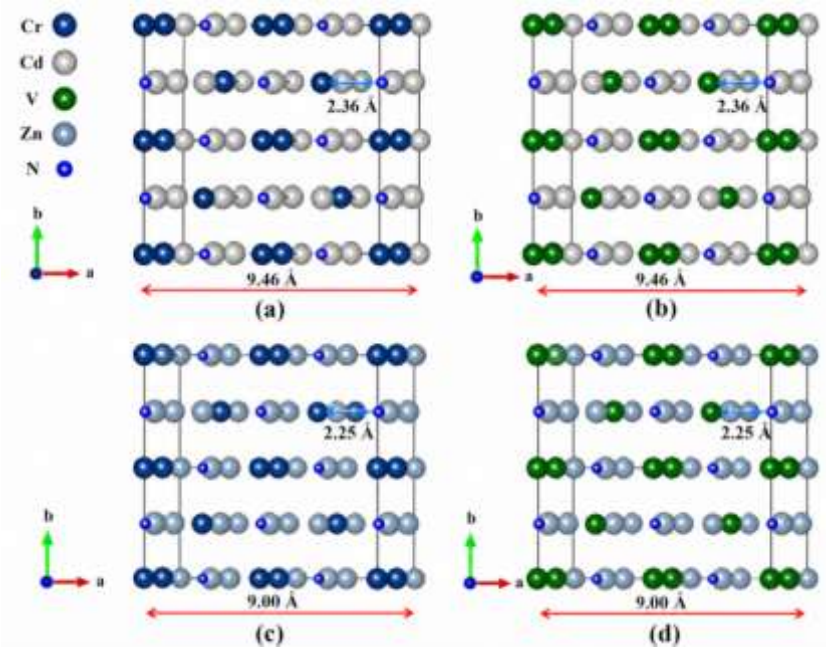

The atomic arrangements of the doped compounds were further analyzed and are illustrated in Fig. 2, where the substitutional positions of Cr and V atoms within the cation sublattice are

clearly shown. The dopant atoms occupy specific lattice sites without inducing noticeable distortion in the crystal structure. Structural relaxation confirms that the cubic symmetry is retained even after replacing Cd and Zn atoms with transition metal dopants.

The stability of these doped systems is strongly influenced by the chosen doping concentration. It is observed that a concentration of 37.5% is sufficient to induce ferromagnetic ordering and enhance half-metallic characteristics. Lower doping concentrations are generally inadequate to produce strong exchange interactions required for half-metallicity. Similar observations have been reported in other transition metal doped nitride systems, where substitutional doping preserves structural symmetry while modifying electronic and magnetic properties [24].
Overall, the volume optimization results confirm that all investigated compounds are energetically stable and maintain their cubic rock salt structure. These optimized geometries provide a reliable basis for subsequent calculations of electronic structure, density of states, and magnetic properties.

4. Band Structure and Density of States (DOS)

The electronic structure of both undoped and transition metal doped CdN and ZnN compounds was analyzed through spin-polarized band structure and density of states (DOS) calculations. These calculations provide detailed insight into the nature of electronic states near the Fermi level and the origin of half-metallicity in the doped systems.

4.1 Undoped CdN and ZnN

The electronic structures of pristine CdN and ZnN were examined to provide a reference for understanding the effects of transition metal doping. Both compounds exhibit semiconducting behavior with narrow band gaps, consistent with previous theoretical and experimental studies [25–27]. The valence band is mainly derived from N-2p states, while the conduction band is dominated by cation s-states.

In CdN, the band gap is relatively small, placing it close to a semimetallic regime, whereas ZnN shows a more pronounced semiconducting character. The difference arises from the position and contribution of cation d-states, which are more localized in ZnN compared to CdN. This electronic structure makes both compounds suitable host materials for inducing spin polarization through transition metal doping.

4.2 Doped CdN and ZnN

The total and partial density of states (DOS) provide detailed insight into the distribution of electronic states and the contribution of different atomic orbitals to the electronic structure. The spin-resolved total DOS for all doped compounds is shown in Fig. 3, while the corresponding partial DOS (PDOS) is presented in Fig. 4.

Fig. 3: Spin-polarized Total density of states (DOS) for (a) $Cd_{0.625}Cr_{0.375}N$, (b) $Cd_{0.625}V_{0.375}N$, (c) $Zn_{0.625}Cr_{0.375}N$, and (d) $Zn_{0.625}V_{0.375}N$.

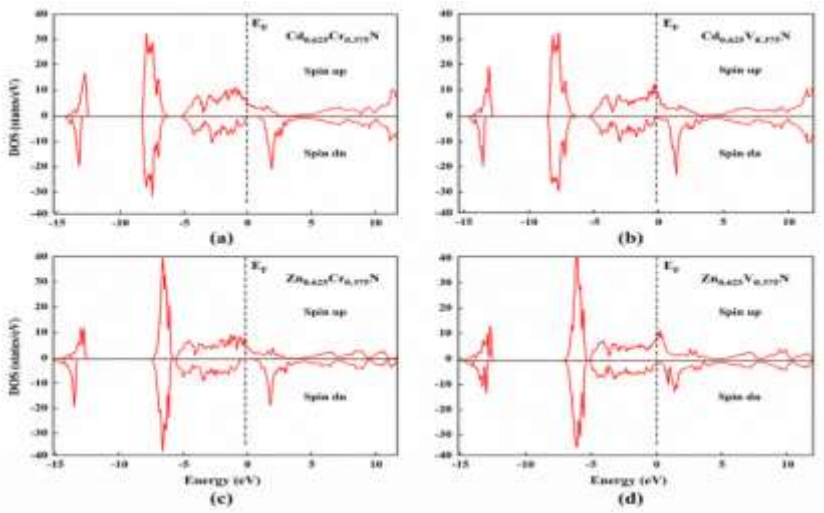

Fig. 4: Spin-resolved projected density of states (PDOS) of $Cd_{1-x}M_xN$ and $Zn_{1-x}M_xN$ (M = Cr, V; x = 0.375): (a, b) M–d and N–p states, (c, d) Cd–d states, and (e, f) Zn–d states.

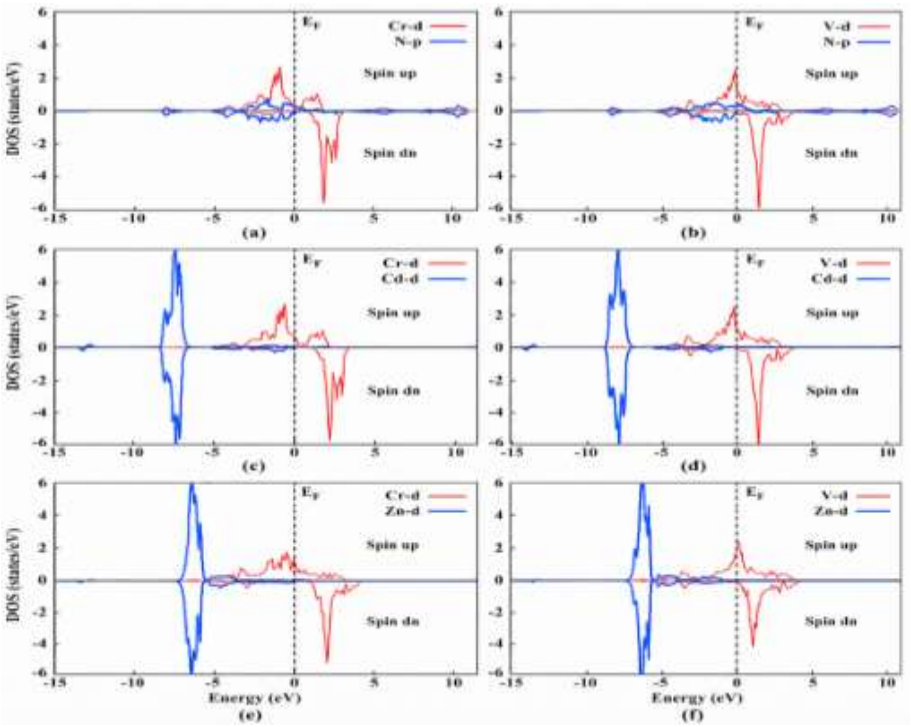

For the Cr-doped compound $Cd_{0.625}Cr_{0.375}N$, the DOS reveals a strong hybridization between Cr-3d states and N-2p states in the energy range from approximately −5 eV to 2 eV. In the spin-up channel, there is a finite density of states at the Fermi level, indicating metallic behavior. In contrast, the spin-down channel exhibits a clear energy gap of about 0.925 eV, confirming the half-metallic nature of the compound. The absence of states at the Fermi level in the minority spin channel results in complete spin polarization.
In $Cd_{0.625}V_{0.375}N$, the hybridization between V-3d and N-2p states is comparatively weaker and both spin channels exhibit finite density of states at the Fermi level. This indicates metallic behavior without the formation of a spin-dependent gap. Although the spin-up channel shows a higher density of states compared to the spin-down channel, the system does not exhibit half-metallicity.

A similar trend is observed for Zn-based compounds. In $Zn_{0.625}Cr_{0.375}N$, the Cr-3d states strongly hybridize with N-2p states, resulting in a finite DOS at the Fermi level in the spin-up channel and a well-defined gap of approximately 1.12 eV in the spin-down channel. This confirms the half-metallic ferromagnetic behavior of the compound. The larger gap compared to the Cd-based system suggests stronger exchange splitting in the Zn host lattice.

In contrast, $Zn_{0.625}V_{0.375}N$ shows metallic behavior in both spin channels, with V-3d states crossing the Fermi level. The absence of a band gap in either spin channel indicates that the compound does not exhibit half-metallicity, although partial spin polarization is present.
The DOS analysis clearly demonstrates that Cr doping induces strong exchange splitting and leads to half-metallicity, whereas V doping results in metallic behavior with reduced spin polarization. The origin of this difference lies in the strength of p-d hybridization and the degree of localization of the transition metal d-states [28–30].

3.3 Band Structure

The spin-resolved electronic band structures of the doped CdN and ZnN compounds provide further confirmation of the half-metallic behavior observed in the DOS analysis. The band structures for Cd-based compounds are shown in Fig. 5, while those for Zn-based compounds are presented in Fig. 6.

Fig. 5: Spin-resolved band structure of $Cd_{0.625}Cr_{0.375}N$ and $Cd_{0.625}V_{0.375}N$.

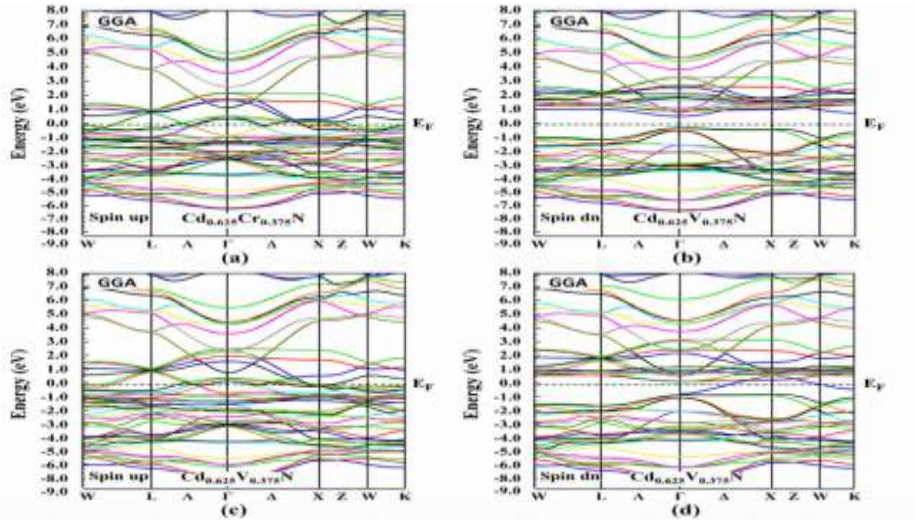

Fig. 6: Spin-resolved band structure of $Zn_{0.625}Cr_{0.375}N$ and $Zn_{0.625}V_{0.375}N$.

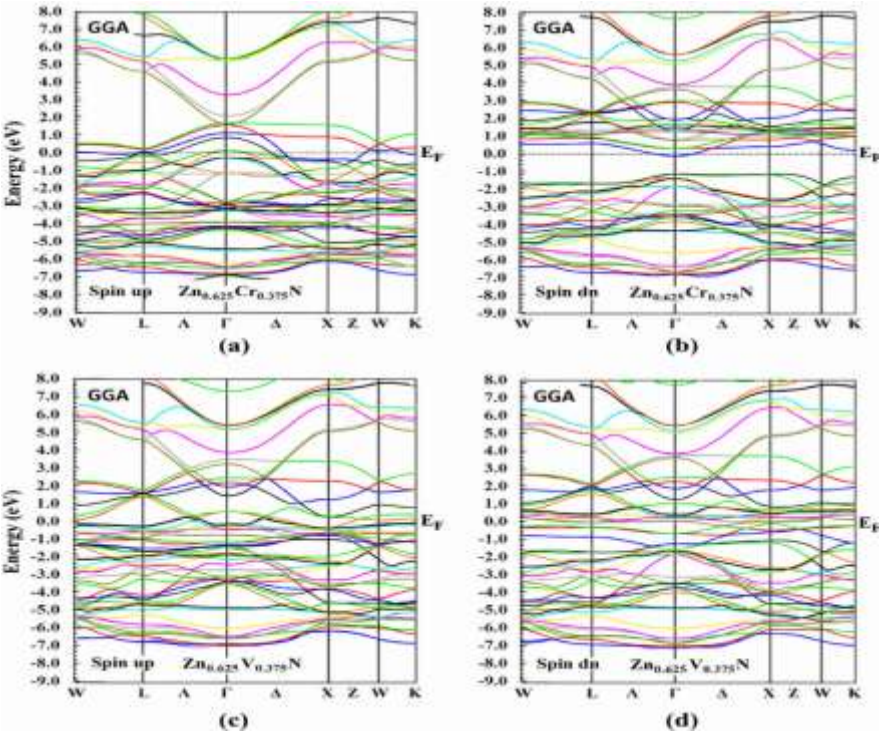

For $Cd_{0.625}Cr_{0.375}N$, the spin-up band structure shows several bands crossing the Fermi level, indicating metallic behavior. In contrast, the spin-down band structure exhibits a clear energy gap of approximately 0.925 eV between the valence band maximum and conduction band minimum along high symmetry directions. This confirms that the compound behaves as a half-metal, with conduction occurring only in one spin channel. In $Cd_{0.625}V_{0.375}N$, both spin-up and

spin-down band structures show bands crossing the Fermi level, indicating metallic behavior in both channels. The absence of a band gap and weak exchange splitting of V-3d states result in the loss of half-metallic characteristics.

For $Zn_{0.625}Cr_{0.375}N$, the spin-up band structure again shows metallic behavior with bands crossing the Fermi level. However, in the spin-down channel, a significant band gap of approximately 1.12 eV is observed. This confirms the half-metallic nature of the compound and indicates stronger exchange splitting compared to the Cd-based counterpart.

In contrast, $Zn_{0.625}V_{0.375}N$ exhibits metallic behavior in both spin channels, with bands crossing the Fermi level along multiple high symmetry directions. The lack of a spin-dependent gap confirms that the compound does not exhibit half-metallicity.

The band structure analysis reinforces the conclusions drawn from the DOS results, clearly showing that Cr doping leads to spin-dependent band gap formation, while V doping results in metallic behavior. The formation of a band gap in one spin channel is a direct consequence of exchange splitting and p-d hybridization, which are stronger in Cr-doped systems.

3.4 DFT+U Calculations

To accurately describe the localized nature of transition metal d-electrons, the electronic structures of Cr-doped CdN and ZnN were further investigated using the DFT+U approach. The inclusion of on-site Coulomb interaction is essential to correct the underestimation of electron correlation effects inherent in standard GGA calculations, particularly for systems containing partially filled 3d orbitals [28]. In the present study, Hubbard U values of 2.3 eV, 5.0 eV, and 6.0 eV were applied to the Cr-3d states, while the exchange parameter J was taken as zero.

The spin-resolved band structures calculated using GGA+U for $Cd_{0.625}Cr_{0.375}N$ and $Zn_{0.625}Cr_{0.375}N$ are shown in Fig. 7 to Fig. 9, corresponding to different values of the Hubbard U parameter. At U = 2.3 eV, the band structures exhibit only minor changes compared to the GGA results, with the spin-down band gap remaining nearly unchanged. This indicates that weak on-site Coulomb interaction has a limited effect on the electronic structure.

Fig. 7: Spin-resolved band structure of $Cd_{0.625}Cr_{0.375}N$ and $Zn_{0.625}Cr_{0.375}N$ in spin-up and spin-down directions calculated using GGA+U with U=2.3 eV.

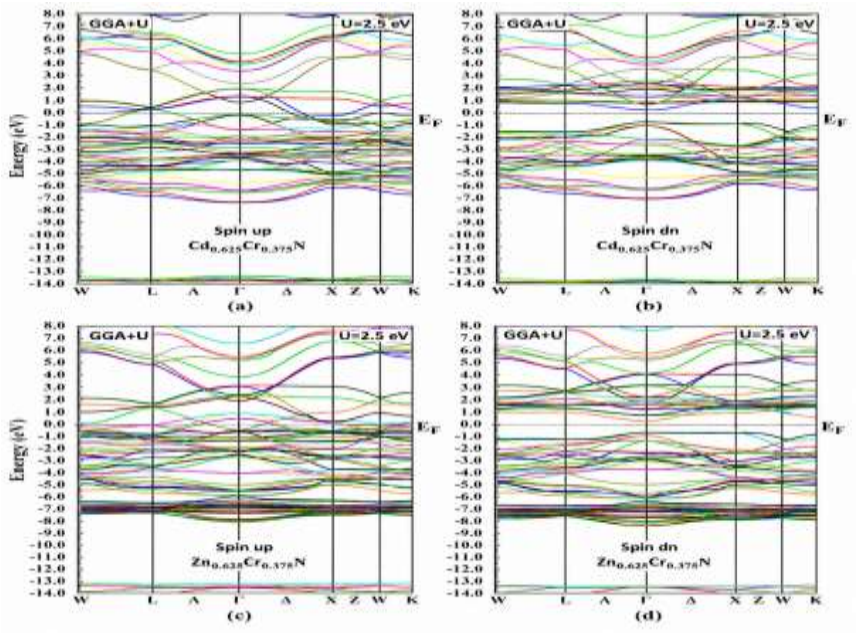

Fig. 8: Spin-resolved band structure of $Cd_{0.625}Cr_{0.375}N$ and $Zn_{0.625}Cr_{0.375}N$ in spin-up and spin-down directions calculated using GGA+U with U=5.0 eV.

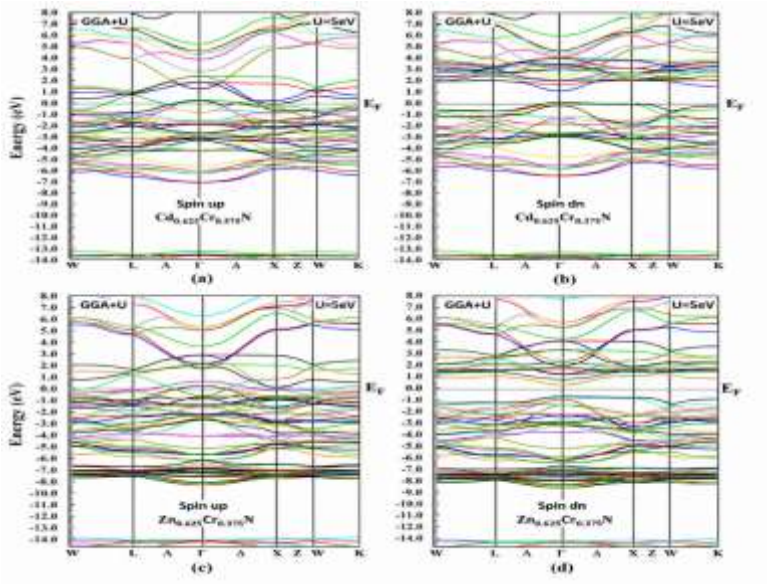

Fig. 9: Spin-resolved band structure of $Cd_{0.625}Cr_{0.375}N$ and $Zn_{0.625}Cr_{0.375}N$ in spin-up and spin-down directions calculated using GGA+U with U=6.0 eV.

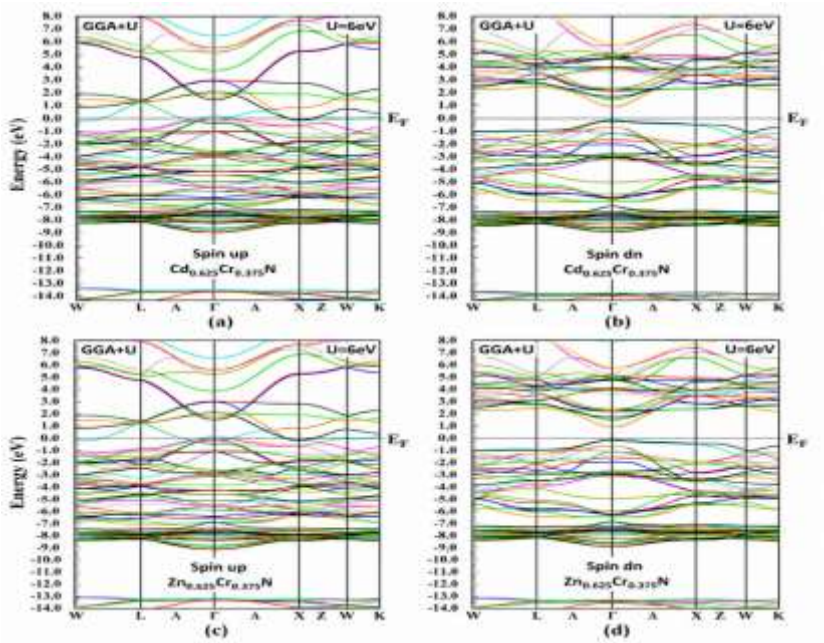

As the Hubbard U value increases to 5.0 eV, a noticeable enhancement in the band gap is observed in the spin-down channel for both compounds. In $Cd_{0.625}Cr_{0.375}N$, the increase in band gap is moderate, whereas in $Zn_{0.625}Cr_{0.375}N$, the increase is more significant, indicating stronger localization of Cr-3d electrons in the Zn-based system. This behavior arises from the increased separation between occupied and unoccupied d-states due to enhanced Coulomb repulsion.

At a higher value of U=6.0 eV, the band gap in the spin-down channel further increases, reaching approximately 1.9 eV for both compounds. The progressive increase in band gap with increasing U confirms that electron correlation plays a crucial role in determining the electronic structure and half-metallic behavior of these materials. Importantly, the metallic nature of the spin-up channel remains unaffected, thereby preserving the half-metallic character.

The effect of the Hubbard U parameter can be understood in terms of enhanced localization of Cr-3d electrons, which leads to stronger exchange splitting and increased separation between valence and conduction bands in the minority spin channel. Similar trends have been reported in transition metal doped semiconductors, where the inclusion of on-site Coulomb interaction improves the description of electronic and magnetic properties [29].

Overall, the DFT+U results demonstrate that Cr-doped CdN and ZnN maintain their half-metallic nature across a range of U values. The increase in the minority spin band gap with U enhances the robustness of half-metallicity, making these materials more suitable for spintronic applications requiring stable and high spin polarization.

3.5 Magnetic Properties

The magnetic properties of Cr- and V-doped CdN and ZnN compounds were investigated through spin-polarized calculations. The introduction of transition metal dopants into the non-

magnetic host lattices induces magnetic ordering due to exchange interactions between localized d-electrons and the surrounding lattice.

The calculated total magnetic moments per supercell for all doped compounds are summarized in Table 2. It is observed that all systems exhibit finite magnetic moments, confirming the emergence of ferromagnetic behavior upon doping. Among the studied compounds, Cr-doped systems show significantly higher magnetic moments compared to V-doped systems, indicating stronger exchange interactions associated with Cr-3d electrons.

For $Cd_{0.625}Cr_{0.375}N$, the total magnetic moment is calculated to be 6.38 μB per supercell, corresponding to approximately 3.19 μB per formula unit. In contrast, $Cd_{0.625}V_{0.375}N$ exhibits a much lower magnetic moment of 2.18 μB per supercell (1.09 μB per formula unit). A similar trend is observed in Zn-based compounds, where $Zn_{0.625}Cr_{0.375}N$ shows a magnetic moment of 4.05 μB per supercell (2.03 μB per formula unit), while $Zn_{0.625}V_{0.375}N$ exhibits a significantly smaller value of 1.01 μB per supercell.

The relatively large magnetic moments in Cr-doped systems are primarily attributed to the strong contribution of Cr-3d states, which undergo significant exchange splitting. In contrast, V-doped systems exhibit weaker exchange interactions, leading to reduced magnetic moments and absence of half-metallicity. This difference is consistent with the electronic structure analysis, where Cr-doped systems exhibit strong spin polarization, while V-doped systems remain metallic in both spin channels.

The effect of electron correlation on magnetic properties was further examined using the GGA+U approach. It is observed that the magnetic moments of Cr-doped compounds increase with increasing Hubbard U, as shown in Table 2. For $Cd_{0.625}Cr_{0.375}N$, the magnetic moment increases from 6.38 μB (GGA) to 8.50 μB at U=6.0 eV. Similarly, $Zn_{0.625}Cr_{0.375}N$ shows an increase from 4.05 μB to 5.30 μB with increasing U. This trend can be attributed to enhanced localization of d-electrons, which strengthens exchange splitting and magnetic ordering [30].

A comparison with other transition metal doped nitride systems reported in the literature shows similar magnitudes of magnetic moments. For instance, Fe- and Mn-doped GaN and InN systems exhibit magnetic moments in the range of 3 - 4 μB per dopant atom, depending on concentration and computational method [31]. Although direct comparison is limited due to differences in doping concentration and host materials, the present results fall within the expected range for transition metal doped semiconductors.

Overall, the magnetic analysis confirms that Cr-doped CdN and ZnN exhibit strong ferromagnetism with enhanced magnetic moments, while V-doped systems show comparatively weaker magnetic behavior. The increase in magnetic moment with Hubbard U further highlights the importance of electron correlation effects in accurately describing the magnetic properties of these systems.

Table 2: Calculated magnetic moments (μB per supercell) of doped CdN and ZnN

Sl. No.	Compound	GGA	GGA+U (U = 2.3 eV)	GGA+U (U = 5.0 eV)	GGA+U (U = 6.0 eV)
1	$Cd_{0.625}Cr_{0.375}N$	6.38	7.47	8.48	8.50
2	$Cd_{0.625}V_{0.375}N$	2.18	-	-	-
3	$Zn_{0.625}Cr_{0.375}N$	4.05	4.17	4.98	5.30
4	$Zn_{0.625}V_{0.375}N$	1.01	-	-	-

7. Conclusions

In this work, the electronic and magnetic properties of Cr- and V-doped CdN and ZnN were systematically investigated using first-principles calculations within the GGA and GGA+U frameworks. The structural analysis confirmed that all doped compounds remain stable in the cubic rock salt phase, with only minor changes in lattice parameters upon doping. The electronic structure results revealed that Cr-doped CdN and ZnN exhibit half-metallic ferromagnetism, characterized by metallic behavior in the spin-up channel and a finite band gap in the spin-down channel, resulting in 100% spin polarization at the Fermi level.

In contrast, V-doped systems show metallic behavior in both spin channels with reduced spin polarization, indicating the absence of half-metallicity. The inclusion of Hubbard U was found to enhance the band gap in the minority spin channel and increase the magnetic moments, highlighting the importance of electron correlation effects. The magnetic analysis further confirmed strong ferromagnetism in Cr-doped systems compared to V-doped counterparts. Overall, the results demonstrate that Cr-doped CdN and ZnN are promising candidates for spintronic applications, particularly as efficient spin injectors and spin filters.

References

[1] Žutić, I., Fabian, J., Das Sarma, S. Spintronics: Fundamentals and applications. Rev. Mod. Phys. 76 (2004) 323–410. https://doi.org/10.1103/RevModPhys.76.323

[2] Katsnelson, M.I., Irkhin, V.Y., Chioncel, L., Lichtenstein, A.I., de Groot, R.A. Half-metallic ferromagnets: From band structure to many-body effects. Rev. Mod. Phys. 80 (2008) 315–378. https://doi.org/10.1103/RevModPhys.80.315

[3] de Groot, R.A., Mueller, F.M., van Engen, P.G., Buschow, K.H.J. New class of materials: Half-metallic ferromagnets. Phys. Rev. Lett. 50 (1983) 2024–2027. https://doi.org/10.1103/PhysRevLett.50.2024

[4] Wolf, S.A., Awschalom, D.D., Buhrman, R.A., et al. Spintronics: A spin-based electronics vision for the future. Science 294 (2001) 1488–1495. https://doi.org/10.1126/science.1065389

[5] Dietl, T., Ohno, H., Matsukura, F. Ferromagnetism in dilute magnetic semiconductors. Science 287 (2000) 1019–1022. https://doi.org/10.1126/science.287.5455.1019

[6] Jiang, X., et al. Optical properties of Zn_3N_2 thin films. J. Appl. Phys. 111 (2012) 033709. https://doi.org/10.1063/1.3681296

[7] Zong, F., et al. Structural and optical properties of Zn_3N_2 films. J. Phys. D: Appl. Phys. 39 (2006) 3051–3055. https://doi.org/10.1088/0022-3727/39/14/023

[8] Zhao, Y., et al. Electronic properties of CdN: First-principles study. Physica B 405 (2010) 4522–4525. https://doi.org/10.1016/j.physb.2010.08.022

[9] Sato, K., Katayama-Yoshida, H. Material design for transparent ferromagnets with ZnO-based magnetic semiconductors. Jpn. J. Appl. Phys. 40 (2001) L334–L336. https://doi.org/10.1143/JJAP.40.L334

[10] Kanoun, M.B., Goumri-Said, S., Merad, G., Aourag, H. First-principles study of magnetic properties of doped semiconductors. J. Magn. Magn. Mater. 290–291 (2005) 118–122. https://doi.org/10.1016/j.jmmm.2004.11.358

[11] Pardo, V., Pickett, W.E. Electron correlation effects in transition metal oxides. Phys. Rev.

B 80 (2009) 054415. https://doi.org/10.1103/PhysRevB.80.054415
[12] Dudarev, S.L., Botton, G.A., Savrasov, S.Y., Humphreys, C.J., Sutton, A.P. Electron-energy-loss spectra and the structural stability of nickel oxide. Phys. Rev. B 57 (1998) 1505–1509. https://doi.org/10.1103/PhysRevB.57.1505
[13] Hohenberg, P., Kohn, W. Inhomogeneous electron gas. Phys. Rev. 136 (1964) B864–B871. https://doi.org/10.1103/PhysRev.136.B864
[14] Kohn, W., Sham, L.J. Self-consistent equations including exchange and correlation effects. Phys. Rev. 140 (1965) A1133–A1138. https://doi.org/10.1103/PhysRev.140.A1133
[15] Blaha, P., Schwarz, K., Madsen, G.K.H., Kvasnicka, D., Luitz, J. WIEN2k: An augmented plane wave + local orbitals program for calculating crystal properties. (2001).
[16] Madsen, G.K.H., Blaha, P., Schwarz, K., Sjöstedt, E., Nordström, L. Efficient linearization of the augmented plane-wave method. Phys. Rev. B 64 (2001) 195134. https://doi.org/10.1103/PhysRevB.64.195134
[17] Schwarz, K., Blaha, P., Madsen, G.K.H. Electronic structure calculations of solids using WIEN2k package. Comput. Phys. Commun. 147 (2002) 71–76. https://doi.org/10.1016/S0010-4655(02)00206-0
[18] Perdew, J.P., Zunger, A. Self-interaction correction to density-functional approximations. Phys. Rev. B 23 (1981) 5048–5079. https://doi.org/10.1103/PhysRevB.23.5048
[19] Perdew, J.P., Burke, K., Ernzerhof, M. Generalized gradient approximation made simple. Phys. Rev. Lett. 77 (1996) 3865–3868. https://doi.org/10.1103/PhysRevLett.77.3865
[20] Perdew, J.P., Burke, K., Ernzerhof, M. Generalized gradient approximation made simple (Erratum). Phys. Rev. Lett. 78 (1997) 1396. https://doi.org/10.1103/PhysRevLett.78.1396
[21] Monkhorst, H.J., Pack, J.D. Special points for Brillouin-zone integrations. Phys. Rev. B 13 (1976) 5188–5192. https://doi.org/10.1103/PhysRevB.13.5188
[22] Birch, F. Finite elastic strain of cubic crystals. Phys. Rev. 71 (1947) 809–824. https://doi.org/10.1103/PhysRev.71.809
[23] Anisimov, V.I., Zaanen, J., Andersen, O.K. Band theory and Mott insulators: Hubbard U correction. Phys. Rev. B 44 (1991) 943–954. https://doi.org/10.1103/PhysRevB.44.943
[24] Sato, K., Katayama-Yoshida, H. First-principles materials design for semiconductor spintronics. Semicond. Sci. Technol. 17 (2002) 367–376. https://doi.org/10.1088/0268-1242/17/4/304
[25] Zhao, Y., et al. First-principles study of electronic properties of CdN. Physica B 405 (2010) 4522–4525. https://doi.org/10.1016/j.physb.2010.08.022
[26] Jiang, X., et al. Optical properties and band gap of Zn_3N_2 thin films. J. Appl. Phys. 111 (2012) 033709. https://doi.org/10.1063/1.3681296
[27] Zong, F., et al. Structural and optical properties of Zn_3N_2 films. J. Phys. D: Appl. Phys. 39 (2006) 3051–3055. https://doi.org/10.1088/0022-3727/39/14/023
[28] Dudarev, S.L., Botton, G.A., Savrasov, S.Y., Humphreys, C.J., Sutton, A.P. Electron-energy-loss spectra and the structural stability of strongly correlated systems. Phys. Rev. B 57 (1998) 1505–1509. https://doi.org/10.1103/PhysRevB.57.1505
[29] Anisimov, V.I., Aryasetiawan, F., Lichtenstein, A.I. First-principles calculations of

electronic structure with strong correlations. J. Phys.: Condens. Matter 9 (1997) 767–808. https://doi.org/10.1088/0953-8984/9/4/002

[30] Doumi, B., et al. Magnetic properties of Fe-doped GaN and InN. J. Magn. Magn. Mater. 324 (2012) 332–336. https://doi.org/10.1016/j.jmmm.2011.08.021

[31] Kanoun, M.B., et al. First-principles study of Mn-doped semiconductors. J. Magn. Magn. Mater. 290–291 (2005) 118–122. https://doi.org/10.1016/j.jmmm.2004.11.358